Magneto Collective Excitations of Armchair Carbon Nanotubes

Chih-Wei Chiu[1], F. L. Shyu[2], C. P. Chang[1], R. B. Chen[1], and M. F. Lin[1]

[1]*Department of Physics, National Cheng Kung University, Tainan 701, Taiwan*
[2] *Department of Physics, Chinese Military Academy, Kaohsiung 830, Taiwan*

An armchair carbon nanotube can exhibit interesting excitation properties, since the transferred momentum (q) and angular momentum (L) during the e-e interactions are conserved on a cylindrical surface [1-2]. The low-frequency electronic excitations of L=0 are mainly determined by the $p\pi$ orbitals [2]. Here the sp^3 Slater-Koster tight-binding model and the random-phase approximation (RPA) are, respectively, used to study the magneto band structures and electronic excitations. Also noticed that the previous study uses the tight-binding model only with the single $2p_z$ orbital [3-6]. Our study shows that the magnetic field and the temperature would induce the novel magnetoplasmons. The resonant inelastic light-scattering measurements [7-9] are available in testing the predicted results.

Figure 1 presents the low energy bands of the (10,10) armchair nanotube. At ϕ=0 (Fig. 1(a)), the linear valence and conduction bands of J=10 just intersect each other at E_F. This system is a gapless metal. An energy gap E_g will open as ϕ increases from zero, as shown in Fig. 1(b) at ϕ=0.01 and α=0°. E_g grows in the further increase of ϕ, e.g., Fig. 1(c) at ϕ=0.02 and α=0°. On the other hand, E_g decreases as the direction of magnetic field gradually deviates from the nanotube axis, e.g., Fig. 1(d) at α=30° and Fig. 1(e) at α=60°. It should be noticed that at α=90°, an armchair nanotube remains metallic (Fig. 1(f)). The linear energy bands are almost the same with those at ϕ=0 (Fig. 1(a)).

The imaginary part of the dielectric function of the (10,10) armchair nanotube is shown in Fig. 2(a) at q=1, ϕ=0.02, and various α's. ε_2 exhibits a prominent peak at the single-particle excitation energy ω_{ex}. The real part of the dielectric function, as shown in Fig. 2(b), drastically changes from a positive value to a negative value at ω_{ex} and then approaches to zero. The zero ε_1 and the small ε_2 would lead to collective excitations (plasmon). The loss function, Im[-1/ε], describes the screened excitation spectrum. It is shown in Fig. 3(a) at q=1, T=0, α=0°, and different ϕ's. There is a pronounced peak in each spectrum. It is identified as the interband collective excitations (the first plasmon) of the low energy carriers. The plasmon frequency clearly increases as ϕ grows. This result directly reflects the variation of the energy gap or the single-particle energy with ϕ (Figs. 1(a)-1(c)). However, the strength of plasmon exhibits the opposite behavior. It is dependent on the single-particle excitations or the Landau damping. The direction of magnetic field also has a strong effect on the loss spectrum, as shown in Fig. 3(b) at ϕ=0.02 and different α's. The plasmon at α=90° is the interband and intraband magnetoplasmon. The strength of plasmon (the plasmon frequency) is getting strong (low) in the increasing of α's.

Temperature can make electrons occupy conduction bands and valence bands. In addition to the interband excitations, it induces the intraband excitations, the $c\rightarrow c$ and $v\rightarrow v$ excitations. Two kinds of magnetoplasmon peaks exist in the loss spectra at finite temperature, as shown in Fig. 3(c) at ϕ=0.02, α=0°, and various T's. The intraband magnetoplasmon (the second plasmon) has lower frequency. The increase of free carriers in the same bands makes the intraband magnetoplasmon enhance frequency and strength. The frequency of the interband magnetoplasmon is thus reduced by temperature. The effect of temperature becomes weak, when the direction of magnetic field gradually approaches to the radial direction (Fig. 3(d)). The peak of the intraband magnetoplasmon is replaced by that of the intraband and interband magnetoplasmon at α=90°; that is, the intraband magnetoplasmon and the interband magnetoplasmon are combined into the intraband and interband magnetoplasmon there. Moreover, this plasmon is almost the same with the interband plasmon at ϕ=0 (Fig. 3(a)), or the interband and intraband magnetoplasmon at (T=0, ϕ=0.02, α=90°) (Fig.3(b)). The two main causes are discussed earlier in the part of ε_2. It is deduced that the temperature-dependence (flux-dependence) of electronic excitations is negligible at ϕ=0, or at α=90° and ϕ<0.1 ϕ_0 (at α=90° and ϕ<0.1 ϕ_0). The low-frequency excitation properties in a metallic armchair carbon nanotube does not depend on temperature and flux.

The armchair carbon nanotubes exhibits very rich electronic excitation spectrum. The dependence on the magnetic flux (ϕ), the direction (α) of magnetic field, and the temperature (T) is novel. Each nanotube exhibits one interband magnetoplasmon at low temperature, when the magnetic field is not perpendicular to the nanotube axis. The plasmon frequency decreases (increases) with α (ϕ), while the strength of plasmon exhibits the opposite behavior. One interband and intraband magnetoplasmon can exist at α=90°, and it is almost the same with that in the absence of ϕ. The temperature can induce

one intraband magnetoplasmon and reduce the frequency of the interband magnetoplasmon. The new plasmon is absent at low T, or at high T and largeα. The T -dependence is negligible for the interband and intraband magnetoplasmon at α=90° or the plasmon at ϕ=0.

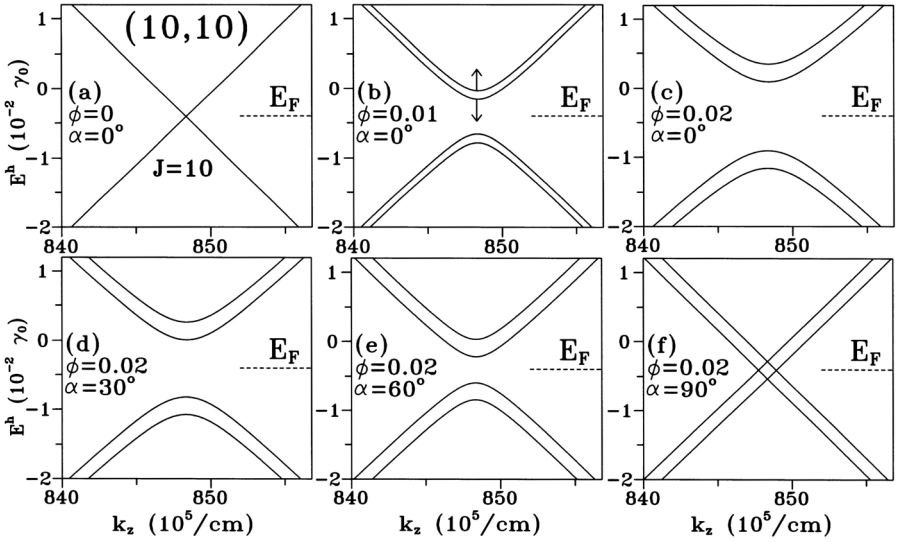

FIG. 1. The low energy bands of J=10 are calculated for the (10,10) armchair nanotube at (a) (ϕ=0, α=0°) , (b) (ϕ=0.01, α=0°), (c) (ϕ=0.02, α=0°), (d) (ϕ=0.02, α=30°), (e) (ϕ=0.02, α=60°); (f) (ϕ=0.02, α=90°). The arrows in (b) represent the directions of spin.

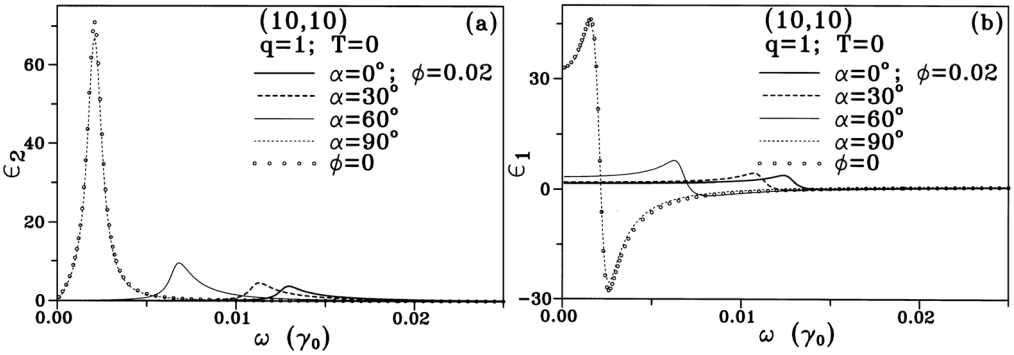

FIG. 2. The imaginary and the real parts of the dielectric function of the (10,10) armchair nanotube are, respectively, shown in (a) and (b) at q=1, T=0, ϕ = 0.02, and different α's. Also shown for comparison are the results at ϕ=0.

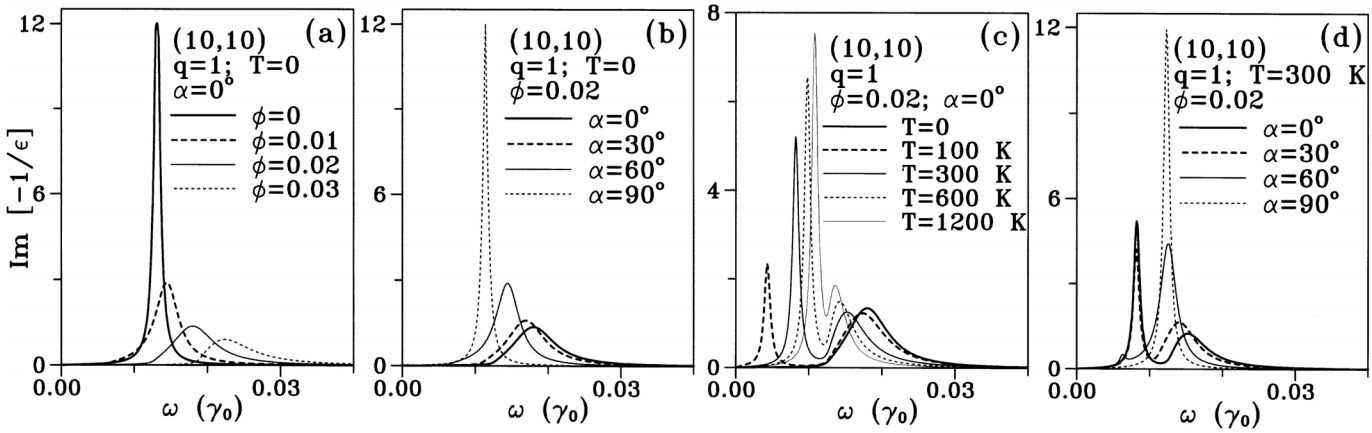

FIG. 3. The loss functions of the (10,10)} armchair nanotube are calculated at (a) q=1, T=0, α=0°; different ϕ's, (b) q=1, T=0, ϕ=0.02; different α's, (c) q=1, ϕ=0.02, α=0°; different T's, and (d) q=1, T=300 K, ϕ=0.02; different α's,

References
[1] M. F. Lin, and K. W. -K. Shung, Phys. Rev. B **47**, 6617(1993); **48**, 5567 (1993).
[2] M. F. Lin, D. S. Chuu, and K. W. -K. Shung, Phys. Rev. B **56**, 1430 (1997).
[3] H. Ajiki, and T. Ando, J. Phys. Soc. Jpn. **62**, 1255 (1993).
[4] H. Ajiki, and T. Ando, J. Phys. Soc. Jpn. **62**, 2470 (1993).
[5] R. Saito *et al*., Phys. Rev. B **50**, 14698 (1994); ibid, **53**, 10408 (Errata; 1996).
[6] S. Roche, G. Dresselhaus, M. S. Dresselhaus, and R. Saito, Phys. Rev. B **62**, 16092 (2000).
[7] A. R. Goni *et al*., Phys. Rev. Lett. **67**, 3298 (1991).
[8] R. Strenz *et al*., Phys. Rev. Lett. **73**, 3022 (1994).
[9] E. Ulrichs *et al*., Phys. Rev. B **56**, 12760 (1997)